

# Design and analysis of embedded flexible packages for wearable device wireless power transfer scheme

Seung Taek Jeong, Su Bin Kim, Shin Young Park, and Joung Ho Kim  
 School of Electrical Engineering, Korea Advanced Institute of Science and Technology University  
 E-mail: seungtaek@kaist.ac.kr

**Abstract** -In this paper, we introduce a wireless power transfer (WPT) scheme using flexible coils and electronic circuits for wearable devices and future flexible devices. Recently, a flexible wearable market is rapidly growing and much effort is made to transform rigid devices into flexible devices. The reason is to provide the comfortable user environment. To realize the flexible devices, electronic circuits must be flexible. Therefore, we designed the voltage-controlled oscillator to analyze the oscillation characteristics with the bending radius. In this paper, we will discuss about a WPT scheme to deliver power to the VCO and designing process of the VCO by considering the effect of thin silicon substrate. To design the VCO, we used SK-Hynix 350 nm CMOS process.

**Keywords**—Embedded packages, Flexible chip, Flexible printed circuit board, Wireless power transfer, Voltage-controlled oscillator

## I. INTRODUCTION

Wireless power transfer technology is very powerful methods to transfer power from one device to another device through an air space without any wired connection [1]. This technology is widely used in applications ranging from low power wearable devices to high power transportation [2], [3]. Especially, the WPT technology on a wearable device provides several useful functions. Firstly, the device can be protected from water or dust by removing power connectors on the surface. Secondly, any mechanical damage such as wear and tear can be removed by avoiding mechanical contacts between power connectors. Moreover, the wearable devices can be easily charged up by simply placing the devices on a wireless charging platform. However, the conventional wireless charging technology has several limitations. In the existing wearable devices, the wireless charging scheme is implemented in the flat or rigid surface of the device. This scheme increases the size of the devices and limits the freedom of design.

Fig. 1 shows the concept of the proposed WPT system using flexible coil and circuits. A polyimide substrate will be used to implement the system and face up, face down and

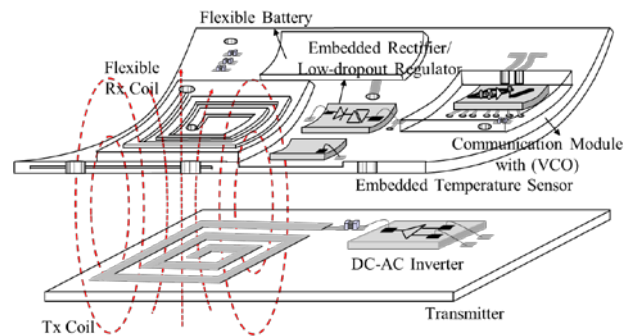


Fig. 1. Proposed wireless power transfer (WPT) scheme using the embedded flexible packages. Power will be delivered through the flexible coils using magnetic field resonance. The rectifier and regulator chips were embedded in the flexible PCB to rectify and regulate the received AC power. Finally, the regulated power will be delivered to the embedded VCO.

embedded packing on the flexible substrate is considered depending on the electronic components. The proposed system enables WPT system with entire flexible environment. The flexible coils were used to deliver the power and rectifier and low-dropout regulator (LDO) were used to rectify and regulate the received AC power for low power application. Finally, the regulate power will be used to supply the VCO. The LC VCO generates the 433 MHz AC voltage at the output. To verify the proposed scheme, power transfer efficiency and voltage transfer ratio between two isolated devices will be analyzed through measurement. More details about the designing process of the VCO with the variation of silicon substrate will be discussed in the later

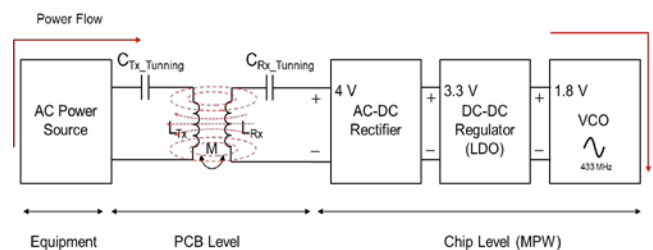


Fig. 2. Overall system block-diagram of the proposed wearable device wireless charging scheme.

section.

Fig. 2 shows the overall system block-diagram of the proposed wearable device wireless charging scheme. On the input side, the AC power will be supplied to excite the Tx coil to produce the magnetic field. The matching capacitor is

a. Corresponding author; joungho@kaist.ac.kr

Manuscript Received Aug. 07, 2018, Revised Aug. 28, 2018, Accepted Sep. 10, 2018

This is an Open Access article distributed under the terms of the Creative Commons Attribution Non-Commercial License (<http://creativecommons.org/licenses/bync/3.0>) which permits unrestricted non-commercial use, distribution, and reproduction in any medium, provided the original work is properly cited.

added in series to minimize the reactive components from the LC resonant circuit. On the Rx side, the Rx coil receives the alternating magnetic field and the voltage will be induced on the Tx side by Faraday’ law [4]. The received AC power will be rectified and regulate to charge up the battery in the device or directly supply the VCO for wireless communication.

II. SIMULATION AND MEASUREMENT RESULTS OF THE PROPOSED WIRELESS POWER TRANSFER SCHEME

To analyze the proposed wearable device wireless charging scheme using the wireless charging receiver, we designed the overall system as shown in Fig.3. The wearable device wireless charging system uses power sources as a commercial electricity and an AC power adapter was used to invert the AC voltage into the 12V DC voltage. The 12 V DC voltage is supplied to an input of the buck-converter that controls the total amount power to be delivered to the wearable device. The regulated DC voltage will be inverted into AC voltage for the WPT using magnetic field resonance. The received AC voltage on the Rx side will be rectified through the full-bridge rectifier. The rectified voltage will be regulated by the LDO to charge up the battery of the device.

We simulated the wearable device wireless charging system to compare with the actual measurement results obtained from the implemented system. Fig. 4 shows the time-domain voltage waveform comparison between the model parameter based simulation and measurement. Due to the parasitic components exist in the system, the measured

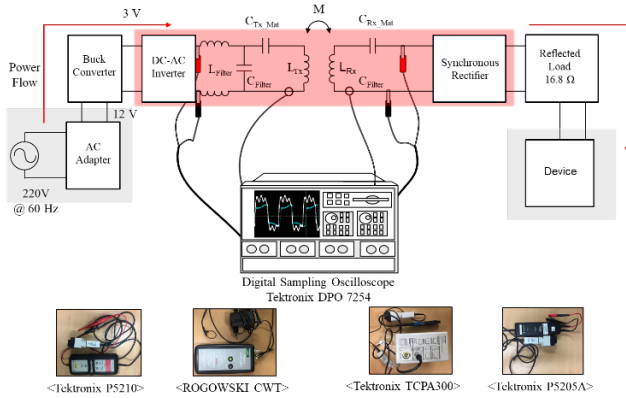


Fig. 3. Measurement setup of Tx and Rx coil voltage and current waveforms using voltage and current probes.

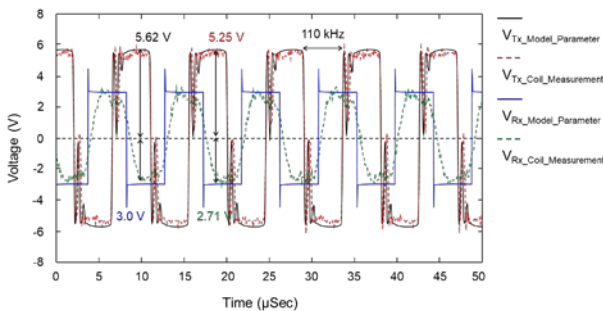


Fig. 4. Comparison between the time-domain voltage waveform simulation and measurement results.

waveforms were degraded. However, the voltage waveforms show the good correlation between the model parameter based simulation and the measurement. Fig.5 shows the comparison between the simulated current waveforms using with the measurement results. Those current waveforms were captured at the Tx and Rx WPT coils as illustrated in the Fig 3. As the results, the amplitudes and the frequency components of the current waveforms between the model parameter based simulation and the measurement results were correlated well with high precision.

III. FLEXIBLE LC VOLTAGE CONTROLLED OSCILLATOR CHIP DESIGN FOR WIRELESS COMMUNICATION FOR FLEXIBLE WEARABLE DEVICES

In the previous chapter, we discussed the simulation and experiments results for the WPT. In this chapter, we will discuss the flexible chip design of the flexible wearable devices. By using SK Hynix 350 nm CMOS process, we will design and fabricate the flexible WPT Rx module to analyze the effect on the current and voltage waveforms and finally the power transfer efficiency due to the bending of the fabricated ICs on the flexible substrate. Also, for the communication module in the devices, we designed the voltage-controlled oscillator (VCO). The VCO is very sensitive to the external environment such as temperature, humidity, and voltage variation. Due to this behavior, we will analyze the operating frequency of the VCO depending on the mechanical stress. Fig. 6 shows the circuit of the LG -G<sub>M</sub>

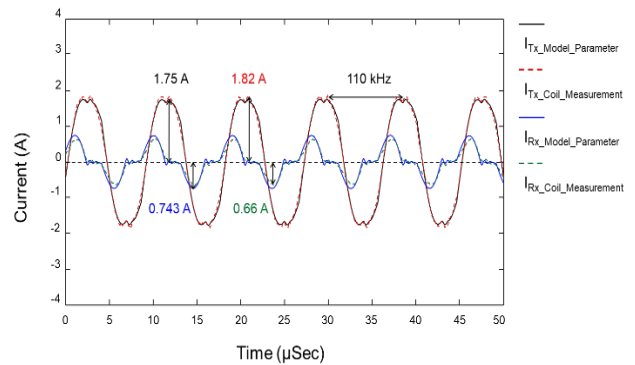


Fig. 5. Comparison between the time-domain current waveform simulation and measurement results.

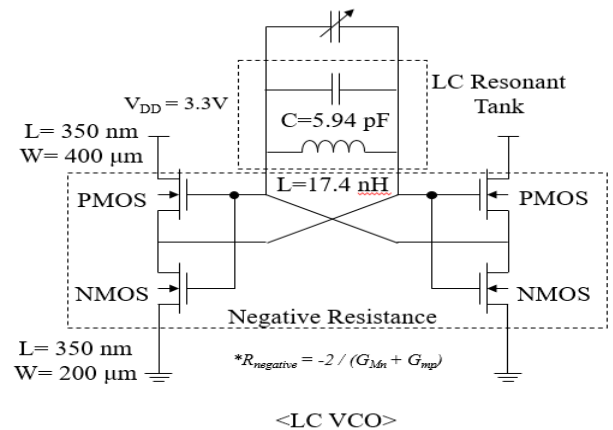


Fig. 6. Designed the LC -G<sub>M</sub> voltage controlled oscillator (VCO) circuit

VCO. The LC resonant tank is used for the oscillation. To avoid the oscillation without damping, the negative resistance circuit is designed. Moreover, the MOS varactor is used to control the operating frequency. However, the SK Hynix 350 nm process does not provide the varactor, therefore, we change the capacitance value to control the operating frequency of the VCO.

For the VCO circuit, an inductor is the main component to oscillate the output waveform. Therefore, we designed the on-chip inductor by changing the designed variables using a 3D EM simulation tool. TABLE I shows the designed on-chip inductor parameters using the 3D EM simulation. Fig. 7 shows the 3D EM simulation result of the designed on-chip inductor. The inductor is designed to achieve the highest Q-factor at 433 MHz for VCO operation. To oscillate the output waveform of the VCO, we used a polysilicon-insulator-polysilicon (PIP) capacitor that can be used in 350 nm process. Once we have designed the on-chip inductor, we simulate the self-impedance  $Z_{self}$  of the inductor with the variation of the silicon substrate thickness as shown in Fig. 8. As the results, the self-inductance of the on-chip inductor varies with the thickness of the silicon substrate. As we increase the thickness of the silicon substrate, the self-resonance frequency of the inductor is reduced. This means the inductance of the capacitance of the inductor can be changed due to the thickness of the silicon substrate.

To realize the flexible devices, we need to make the thinner silicon substrate less than 50 $\mu\text{m}$ . However, the

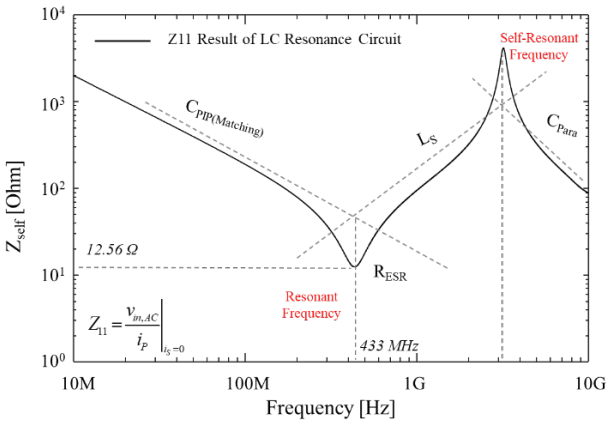


Fig. 7. Self-impedance ( $Z_{self}$ ) 3D EM simulation results of on-chip inductor. We optimize the on-chip inductor to achieve the higher Q-factor at the resonance frequency.

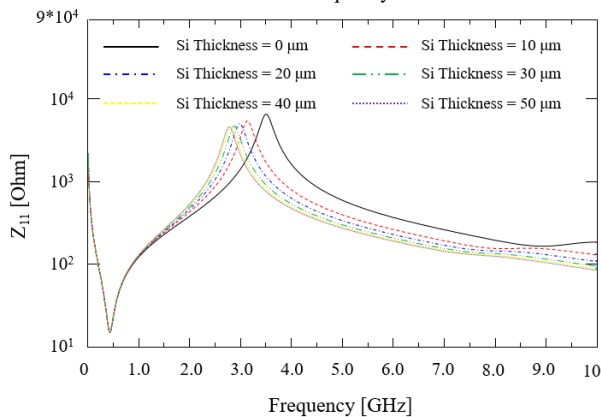


Fig. 8. Changes in the Self-impedance of the on-chip inductor with the variation of the Si substrate thickness.

thickness of the silicon substrate without the back grinding is greater than 100 $\mu\text{m}$ . This means if we design the on-chip inductor with the 100 $\mu\text{m}$  silicon thickness, then the inaccuracy of the VCO resonance frequency will be produced due to the reduction of the thickness of the silicon substrate. During the design process, we need to consider the target thickness of the silicon substrate. In this paper, we set the silicon substrate thickness as 50 $\mu\text{m}$  since it is harder to achieve the thickness less than 50 $\mu\text{m}$  with the diced chips. By considering the above design guides, we apply the designed on-chip inductor using the 3D EM simulation to the actual layout of the on-chip inductor for the VCO.

Fig. 9 shows the voltage waveform output of the designed LC VCO using the Virtuoso circuit simulation tool. The output waveform shows the operating frequency at 433 MHz with the swing voltage of 2.8V. Fig 10 shows the Fast Fourier Transform (FFT) results of the output voltage waveform. As indicated in the graph, the fundamental component is located at 433MHz.

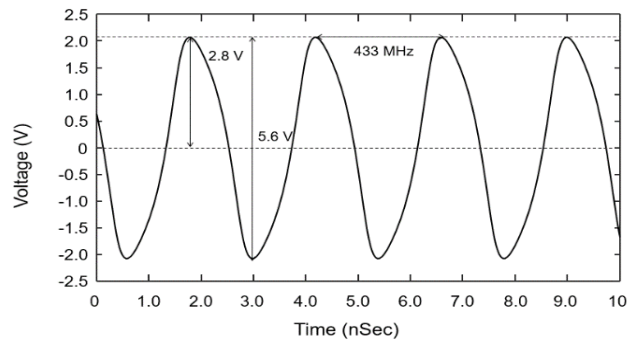


Fig. 9. The output voltage waveform of the designed LC VCO using a circuit simulation tool. The voltage waveform shows the oscillation frequency at 433 MHz

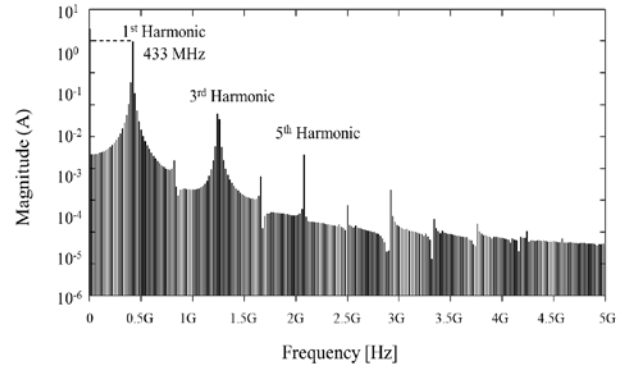


Fig. 10. Fast Fourier Transform (FFT) simulation result of the output voltage waveform.

TABLE I.  
Designed On-chip Inductor Parameters

Design Parameter	Value
Line Width	30 $\mu\text{m}$
.Line Space	1 $\mu\text{m}$
Metal Thickness	0.7 $\mu\text{m}$
Coil Dimension	700 x 700 $\mu\text{m}^2$
Coil Turn	4 turn

IV. MEASUREMENT RESULT OF FABRICATED VOLTAGE CONTROLLED OSCILLATOR

Fig. 11 shows the fabricated on-chip inductor and voltage controlled oscillator (VCO) using SK Hynix 350 nm process. The on-chip inductor pattern for the VCO is designed individually to analyze the inductor characteristic itself since the inductor is one of the main components for the VCO. To measure the designed chip, we designed the probing pads with the 250 μm pitch.

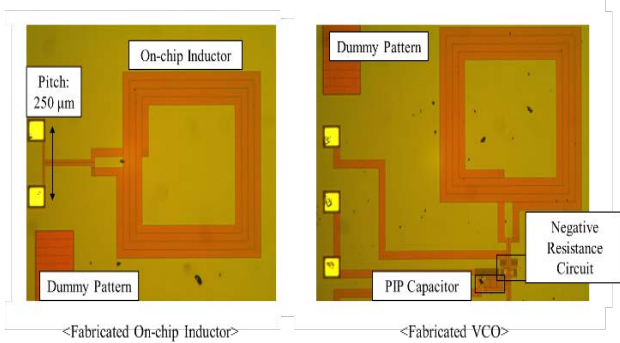


Fig. 11. Fabricated on-chip inductor and voltage controlled oscillator using SK Hynix 0.35 μm process.

Fig. 12 shows the measurement setup of the fabricated on-chip inductor pattern. To measure the inductor pattern, we used the 4-port vector network analyzer (VNA). By using the VNA, we can measure the self-impedance of the inductor. To measure the fabricated VCO, we provide the four probing pads. One pair is used for the input supply and another pair is used for the bias voltage.

When we measure the self-impedance  $Z_{self}$ , we set the target frequency range between 300 kHz and 10 GHz. In this range, we can analyze the resonance of the designed inductor with the matching capacitor for the oscillation and the self-resonance by the parasitic capacitance of the inductor. Fig. 13 indicates the  $Z_{self}$  of the on-chip inductor. The first declining section of the graph indicates the impedance of the matching capacitor. At 433 MHz, the resonance is produced due to design the inductor pattern with the matching capacitor. At this frequency, the only the real term exists since the reactive components of the inductor and the capacitance are canceling each other. Above the 433 MHz, the inclining section indicates the self-inductance of the inductor pattern. At higher frequency region above 3 GHz, the self-resonance is produced due to parasitic capacitance

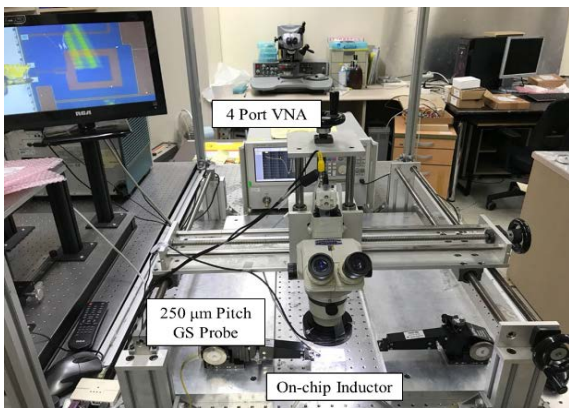


Fig. 12. The measurement setup of the fabricated on-chip inductor pattern using probe station and 4-port VNA

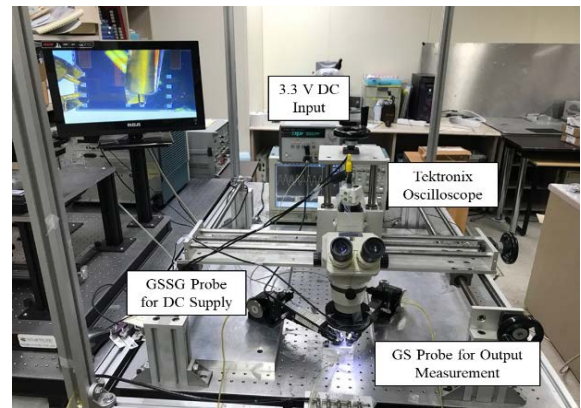


Fig. 14. The measurement setup of the fabricated voltage controlled oscillator (VCO) using the DC supply and oscilloscope.

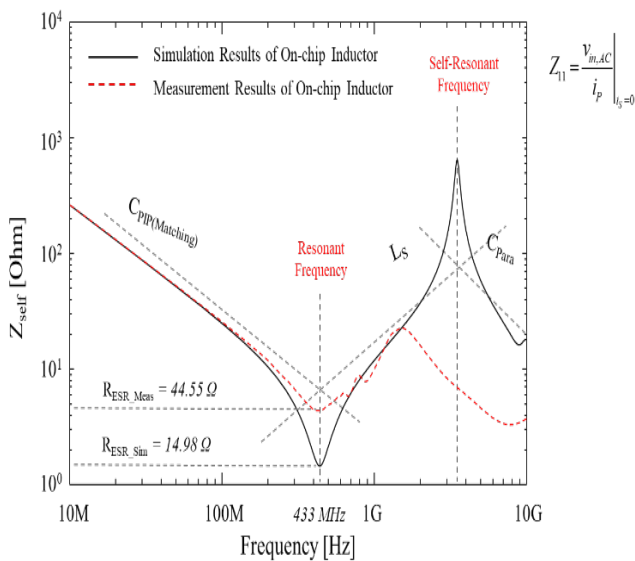


Fig. 13. The self-impedance  $Z_{self}$  measurement result of the fabricated on-chip inductor pattern.

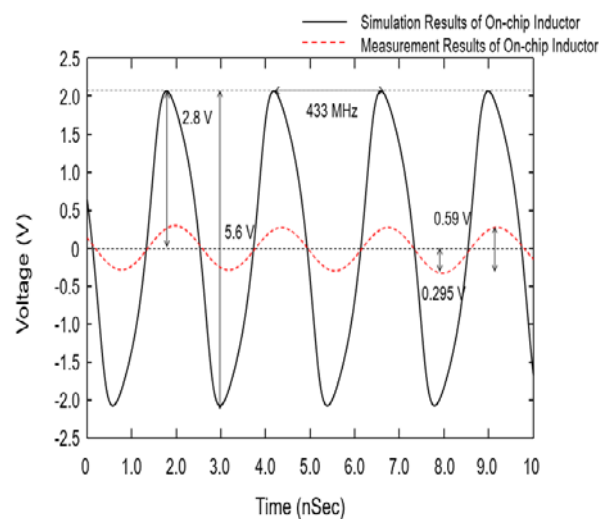


Fig. 15. The voltage waveform measurement result of the fabricated VCO using the Tektronix oscilloscope.

$$Z_{11} = \frac{V_{in,AC}}{I_P} \Big|_{I_S=0}$$

This parasitic capacitance comes from the overlapping region of the top and the bottom metal in the inductor. In the graph, the self-resonance from the measurement result is much lower than the 3D EM simulation results. This means the parasitic capacitance of the actual system is much higher than the simulation results.

Moreover, the measurement result of the equivalent series resistance (ESR) is much higher than the 3D EM simulation results. From the measurement, we achieved the 44.55  $\Omega$  at 433MHz. However, in the simulation result, the ESR is 14.98  $\Omega$ , which is one third of the measurement result. This higher ESR leads the lower Q-factor and degrades the system performance. To avoid the degradation of the Q-factor, we can take out the inductor pattern from the chip to the PCB.

Fig. 14 shows the measurement setup of the fabricated VCO. To measure the fabricated VCO, we supplied 3.3 DC input voltage to operate the VCO. The GSSG probe is used to supply the input voltage and bias voltage. On the output side, the Tektronix oscilloscope is used to measure the output voltage waveform. The GS probe is used to measure the output voltage waveform.

The red line in Fig. 15 shows the measurement result of the VCO. In comparison to the simulation results, the output oscillation is largely decreased. This is due to larger ESR on the on-chip inductor and PIP capacitor for matching. Even the output oscillation is very less, the designed VCO operate at 433 MHz with the peak to peak voltage of 0.59 V. In our research, we will analyze the VCO output depending on the mechanical stress as we bend the flexible PCB with embedded VCO chips.

## V. RESULTS

In this paper, we firstly design the wireless power transfer (WPT) scheme using flexible coils for the flexible wearable devices. From the measurement result, we achieved coil to coil power transfer efficiency of 50.3% where the input power from the transmitter is 3.36 W while the output power from the receiver coil is 1.69 W. For the power transfer efficiency calculation, we used average power calculation using MATLAB tool to calculate the power efficiency from the measured voltage and current waveforms. We also simulated overall DC-DC power transfer efficiency of the proposed system. The input DC power of the buck-converter is 4.67 W and the output DC power delivered at the load is 1.4 W. The power transfer efficiency of the proposed system is 30%. Since the wearable device WPT system delivers very low amount power, the power transfer efficiency can be lower than the high power WPT system due to fixed power losses such as forward voltage drops of the diodes in the rectifier circuit. Compared to the Smartphone wireless charging system which has 50% of power transfer efficiency, 30% power transfer efficiency is not very low.

Once we finish the WPT system design using flexible coils, we designed the LC voltage controlled oscillator (VCO). The input power will be supplied from the WPT system and VCO chip will be flexible for the flexible wearable devices. To design the VCO, we focused on the on-chip inductor design. As the results, as we increase the thickness of the silicon substrate, the self-resonance frequency of the on-chip inductor is decreased. Therefore,

we designed the on-chip inductor at 433 MHz with the thickness of 50  $\mu\text{m}$ . Finally, the fabricated VCO is measured. As the result, the amplitude of the oscillation is largely decreased in comparison to the simulation due to higher equivalent series resistance (ESR) of the on-chip inductor. However, the designed VCO operates at 433 MHz.

## VI. DISCUSSION

To measure the effect of the curvature on the flexible chips, we need to put the fabricated chips on a flexible substrate. In our case, we will use Polyimide substrate, which has good electrical and thermal characteristics. Moreover, the Polyimide has good bending properties. The packaging of flexible circuits on the flexible substrate will be proceeded from Korea Institute of Machinery & Materials (KIMM). Firstly, the fabricated chip will be grinded to obtain the thin flexible chips. The thickness of the chips will be less than 50  $\mu\text{m}$  to have a flexibility. Typically, 25  $\mu\text{m}$  thick chips can have bending radius of 1 cm [5]. In our case, the mechanical stress on the chip due to the bending is not significant since we apply the flexible system on a wearable device, which has bending radius larger than the bending radius of a human wrist. To mount the chip on the PCB, the printing type interconnection technique will be used. This technique allows direct attachment of the flexible chips on the flexible PCB since it can realize the line pattern and pitch less than 50  $\mu\text{m}$ . Therefore, the gap between the PCB level and wafer level can be removed.

## VII. FURTHER WORK

The fabricated VCO will be processed by KIMM to make the thinner silicon substrate. Since the Si substrate is very thin, the fabricated chip can have flexible properties. Through the bulk etching process, the designed chip can have the flexible properties. Once we obtained the flexible VCO chip, we will test the output characteristics of the VCO depending on the silicon thickness. Once the VCO operates with the targeted thickness of the silicon substrate, we will mount on the flexible PCB. Finally, the VCO will be tested under the flexible environment.

## VIII. CONCLUSION

In this paper, we proposed the wireless power transfer scheme using the flexible coils for wearable device and future flexible devices. Currently, the existing wireless power Rx module is implemented on the rigid FR4 PCB. To realize entire flexible device, the Rx chips must be flexible. Therefore, we design the VCO considering the thickness of the silicon substrate for a communication module in the wearable device. The on-chip inductor of the VCO is designed using 3D EM simulation to achieve the higher Q-factor with the target thickness of 50  $\mu\text{m}$ . Finally, the oscillation amplitude is decreased in comparison to the simulation results, the VCO operates correctly at 433 MHz.

## ACKNOWLEDGMENT

This research was supported by "Development of Interconnection System and Process for Flexible Three Dimensional Heterogeneous Devices" funded by MOTIE (Ministry of Trade, Industry and Energy) in Korea and we would like to acknowledge the technical support from ANSYS. This work was supported by the IDEC for device fabrication.

## REFERENCES

- [1] S. Ahn *et al.*, "Low frequency electromagnetic field reduction techniques for the On-Line Electric Vehicle (OLEV)," *2010 IEEE International Symposium on Electromagnetic Compatibility*, Fort Lauderdale, FL, 2010, pp. 625-630.
- [2] Yungtaek Jang and M. M. Jovanovic, "A contactless electrical energy transmission system for portable-telephone battery chargers," in *IEEE Transactions on Industrial Electronics*, vol. 50, no. 3, pp. 520-527, June 2003.
- [3] Chwei-Sen Wang, O. H. Stielau and G. A. Covic, "Design considerations for a contactless electric vehicle battery charger," in *IEEE Transactions on Industrial Electronics*, vol. 52, no. 5, pp. 1308-1314, Oct. 2005.
- [4] H. Kim *et al.*, "Coil Design and Measurements of Automotive Magnetic Resonant Wireless Charging System for High-Efficiency and Low Magnetic Field Leakage," in *IEEE Transactions on Microwave Theory and Techniques*, vol. 64, no. 2, pp. 383-400, Feb. 2016.
- [5] A. Dietzel, J. Brand, J. Vanfleteren, W. Christiaens, E. Bosman, and J. Baets. *System in Foil Technology*. Springer, 2010.



**Seung Taek Jeong** received the B.E. degree in electrical and electronic engineering (with First Class Honors) in 2014 from the University of Auckland, Auckland, New Zealand, the M.S. in electrical engineering in 2017 from Korea Advanced Institute of Science and Technology (KAIST), Daejeon, Korea. He is currently pursuing the Ph.D. degree in electrical engineering from the Korea Advanced Institute of Science and Technology, Daejeon, Korea. His current research interests include design, modeling and experimental verification of wireless power transfer system on a flexible PCB with embedded regulator and RF chips.



**Shin Young Park** received the B.S. and M.S. degrees in electrical engineering from the Korea Advanced Institute of Science and Technology, Daejeon, South Korea, in 2015 and 2017, respectively, where she is currently pursuing the Ph.D. degree with focus on ground integrity analysis in mixed-mode systems.



**Su Bin Kim** received the B.S. and M.S. degrees in electrical engineering from the Korea Advanced Institute of Science and Technology (KAIST), Daejeon, Korea, in 2015 and 2017, respectively, where he is currently pursuing the Ph.D. degree. His current research interests include on-interposer active PDN and integrated voltage regulator design.



**Joung Ho Kim (SM'14-F'16)** received the B.S. and M.S. degrees from Seoul National University, Seoul, Korea, in 1984 and 1986, respectively, and the Ph.D. degree from the University of Michigan, Ann Arbor, MI, USA, in 1993, all in electrical engineering. He joined the Memory Division, Samsung Electronics, Suwon, Korea, in 1994, where he was involved in gigabit-scale DRAM design. In 1996, he joined the Korea Advanced Institute of Science and Technology (KAIST), Daejeon, Korea. He is currently a Professor with the Department of Electrical Engineering, KAIST. He is also the Director of the 3-D Integrated Circuit (IC) Research Center, Daejeon, Korea, supported by SK Hynix Inc., and the Smart Automotive Electronics Research Center, Daejeon, Korea, supported by KET Inc. He has given more than 219 invited talks and tutorials in academia and related industries. In particular, his major research interests include chip-package-printed circuit board (PCB) codesign and cosimulation for signal integrity, power integrity, ground integrity, timing integrity, and radiated emission in 3-D IC, through silicon-via (TSV), and interposer. He has authored or coauthored over 404 technical papers in refereed journals and conference proceedings. He has authored a book titled *Electrical Design of Through-Silicon-Via* (Springer, 2014). His current research interests include electromagnetic compatibility (EMC) modeling, design, and measurement methodologies of 3-D IC, TSV, interposer, system-in-package, multilayer PCB, and wireless power transfer (WPT) technology for 3-D IC, electric vehicles, and mobile phones.